TENSILE BEHAVIOR OF UHPFRC UNDER UNIAXIAL AND BIAXIAL STRESS CONDITIONS

Xiujiang Shen*, Eugen Brühwiler

Division of Maintenance and Safety of Structures (MCS-ENAC), Ecole Polytechnique Fédérale de Lausanne (EPFL), Switzerland
E-mail: xiujiang.shen@epfl.ch, eugen.bruehwiler@epfl.ch

ABSTRACT

The representative characterization of the tensile behavior of strain hardening Ultra High Performance Fiber Reinforced Cementitious Composite (UHPFRC) remains a challenge. Currently, the uniaxial methods (direct tensile test and 4-point bending test) are commonly applied, although the biaxial tensile condition has been widely recognized in most of the UHPFRC applications, e.g. thin UHPFRC element as external reinforcement layer or bridge deck slab. In this paper, the ring-on-ring test on circular slab-like specimens has been developed to determine the equal-biaxial tensile response by means of inverse analysis using 3D finite element method (FEM) models. In addition, direct tensile test (DDT) using dumbbell specimens cut from large square plates and 4PBT (4-point-bending-test) cast in molds were carried out. The representative tensile response from 4PBT was derived through inverse analysis using 2D FEM models. Finally, the corresponding results from different tests under either uniaxial or biaxial stress condition were analyzed and compared in terms of tensile parameters, tensile material law, cracking pattern and energy absorption capacity. The main objective is to examine the tensile performance under uniaxial and biaxial stress conditions, and to propose the most appropriate test method for a given UHPFRC application.

Keywords: Biaxial condition, FEM models, Inverse analysis, Ring-on-ring test, UHPFRC, Uniaxial condition.

1. INTRODUCTION

The tensile response of strain hardening Ultra High Performance Fiber Reinforced Cementitious Composite (UHPFRC) is a fundamental constitutive property. Thus, reliable and representative characterization of this response is necessary for the design of a given UHPFRC application. This can be achieved generally by means of uniaxial test methods, especially the direct tensile test (DTT) and the four-point bending test (4PBT) processed through inverse analysis method. Unfortunately, those tests exhibit considerable scatter and the results are often considered as an upper bound in case of small-scale laboratory specimens, hardly reproducing real situation for design. Most infrastructures, in particular bridge decks and floors, are principally under biaxial stress condition, far from uniaxial stress state [1]. In this context, the actual tensile performance of UHPFRC under biaxial stress condition should be investigated carefully.

In this paper, the ring-on-ring test on circular slab-like specimens has been developed to determine the equal-biaxial tensile response. In addition, direct tensile tests using dumbbell specimens cut from large square plates and 4PBT using small plates cast in molds were carried out. The corresponding tensile response from five DDT, six 4PBT and four ring-on-ring tests are analyzed and compared (Fig.1). The main objective is to examine the differences and relationships of the tensile response of UHPFRC under uniaxial and biaxial stress conditions, and to propose the most appropriate test method to determine the tensile property for a given UHPFRC application.

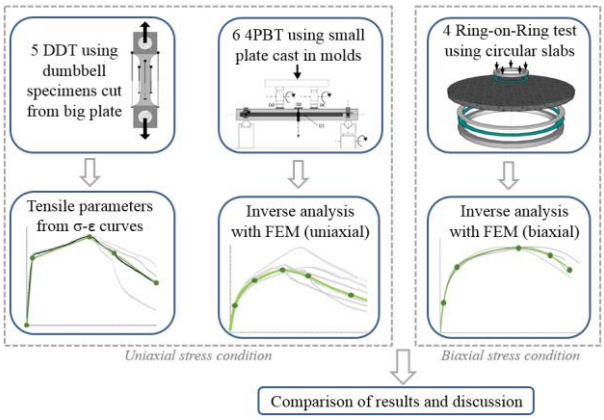

Fig.1 Approach for the comparison of the tensile response of UHPFRC under uniaxial and biaxial stress conditions

2. EXPERIMENTAL PROGRAM

2.1 Ring-on-ring test

The ring-on-ring test method was applied indirectly for the characterization of the tensile behavior under biaxial stress condition, using circular slab-like specimens with a diameter *R=600mm* and a thickness *h=50mm*. This method has been extensively adopted and even standardized by ASTM [2] in the ceramics and glass domain. Recently, this method was modified and validated to measure the biaxial flexure strength of concrete and UHPFRC with several advantages [3–7].

Figure 2(a) shows the full test set-up and devices. The slab was simply supported on a support ring with *R=500 mm*. Loading was imposed by a hydraulic jack acting on the center of slab through a force transmitting ring with *r=150 mm*. All the slabs were subjected to three loading–unloading cycles to *20 kN* with an actuator displacement rate of 1.0 *mm/min*. Afterwards, a monotonic loading with the same displacement rate was applied up to the peak force, followed by a rate of *4.0 mm/min* until the actuator displacement reached *80 mm*.

The slabs were tested with the casting surface facing upwards, allowing the observation of tensile crack propagation on the smooth surface. Before testing, the casting surface was polished and a mortar layer was placed between support ring and bottom surface to level out both surfaces. Two rubber pads (thickness of *10 mm*, *E=500 MPa*) were positioned between the slab surfaces and the two rings to distribute the force evenly.

As illustrated in Figure 2(b), the Digital Image Correlation (DIC) technique was applied to observe the deflection development, strain field and micro-cracking. In addition, several LVDTs were installed on the top surface to measure the deflection. All deflection measurements were performed with respect to the strong floor. The measurement frequency was 5Hz.

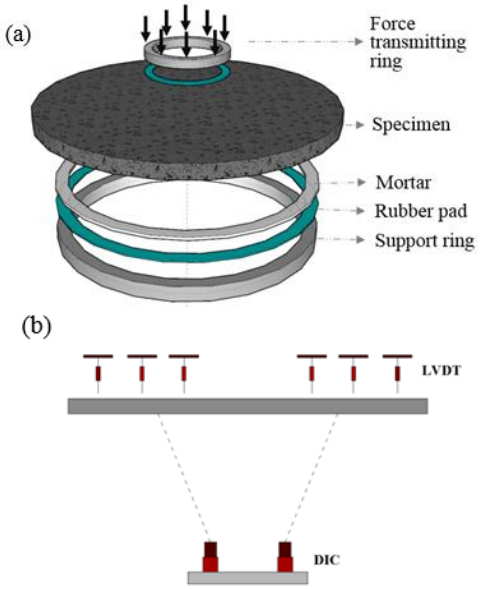

Fig.2 Schematic description of (a) the test setup and (b) instrumentation

2.2 Direct tensile test (DTT)

The dumbbell shaped specimens, with a constant cross section of *80mm* × *50mm* at the central part, were adopted for uniaxial DTT. The geometry of specimen was designed based on the equation of Neuber's spline [8,9]. The five specimens were cut from a large square plate of same thickness and with a casting procedure similar with that for the circular slab-like specimen (Fig. 3a). This allows assessing the variability of tensile behavior in the plate.

Five LVDTs and seven U4 gauges were installed to measure the deformation and crack opening of UHPFRC, as shown in Figure 3(b). The tests were performed using a universal servo-hydraulic testing machine with a capacity of 1000kN, according to SIA 2052 [10].

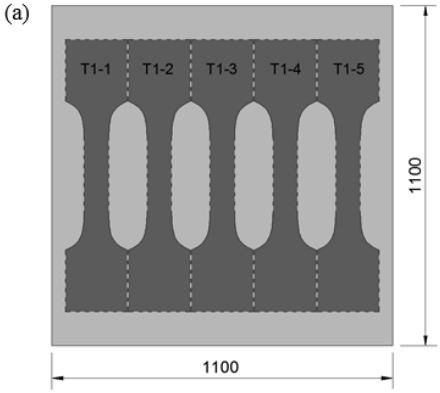

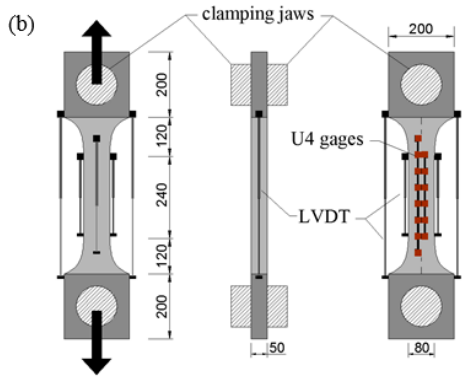

Fig.3 (a) Specimens cut from a large square plate (b) Test setup and instrumentation

2.3 Four-point bending test (4PBT)

In total six small plate specimens with dimension of 50mm × 100mm × 30mm were cast individually in molds. The 4PBT for all specimens were performed on a universal servo-hydraulic testing machine with a capacity of 200kN, according to SIA 2052 [10,11]. The total span of the four-point bending test set up was 420mm (Fig. 4), and the supports allowed free displacement of the specimen along its longitudinal axis. Two transducers placed on a measuring frame on each side of the specimen measured the net deflection in the center of the span. The measurements were taken at a frequency of 5Hz during the test.

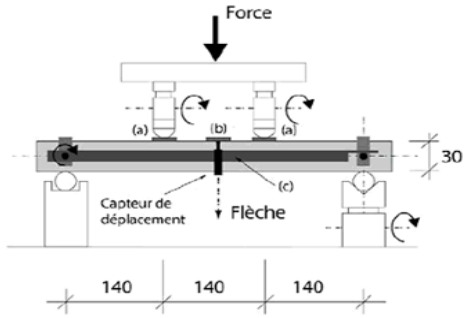

Fig.4 Four-point bending test setup and instrumentation [10]

2.4 Fabrication and curing

The chosen UHPFRC is "Holcim707©", an industrial premix containing 3.8% by volume of 13mm long straight steel fibers with a diameter of 0.175mm.

The UHPFRC was mixed to obtain a batch of 180 liters. The large square plate and circular slab-like specimens were cast in one shot: the fresh UHPFRC was placed at the center and let flown without pulling or vibration. Regarding the small plate specimens for 4PBT, the fresh mixture was poured from one side and let flown. Once the casting was completed, a plastic sheet was pulled over the specimens to allow for auto-curing of the material. The formwork was removed 24 hours after the casting. The specimens were then kept under moist curing conditions for the following seven days, and subsequently stored inside the laboratory until testing.

3. EXPERIMENTAL RESULTS

3.1 Uniaxial tensile response from DDT

The direct tensile stress-strain curves of five specimens from same square plate are shown in Fig.5, respectively; the thick black line corresponds to the average response. The main tensile parameters and average values are given in Table 1, where a considerable scatter can be observed. It is noted that the two specimens (T1-1 and T1-5) from both sides of square plate exhibited more significant tensile performance with remarkable strain hardening behavior, compared with the specimens between them. This can be attributed to the variability of fiber distribution in different specimens depending on the distance from the pouring point, as illustrated in Figure 6. In this case, due to the high fluidity and workability of the UHPFRC "Holcim707©", the fresh mixture flowed freely from the center to the border in radial direction. The flow exerted forces on the fibers. Thus, the fibers tended to align perpendicularly to the flow direction. This can be further confirmed by the positions of the crack of the tested specimens (Fig. 6). Specimens T1-1 and T1-2 have broken in the central part due to relatively uniform fiber distribution along the longitudinal direction, while the remaining specimens have broken in the transition area because of more unfavorable fiber orientation in the loading direction, compared with the other areas in the specimen. This radial distribution mode is consistent with the experimental results from other researchers [12–14].

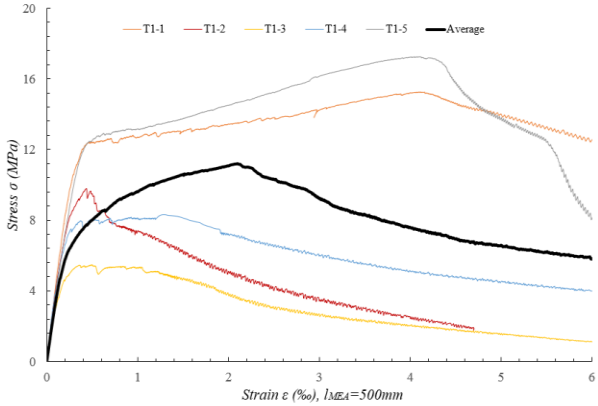

Fig.5 Tensile response from DTT

Tab.1 Tensile parameters from DTT

N°	E_U [MPa]	f_{Ute} [MPa]	f_{Utu} [MPa]	f_{Utu}/f_{Ute}	ε_{Ute} [‰]	ε_{Utu} [‰]
T1-1	46,000	8.1	15.2	1.88	0.20	4.1
T1-2	44,000	6.1	9.7	1.60	0.16	0.4
T1-3	43,000	3.8	5.5	1.44	0.14	0.5
T1-4	45,000	5.7	8.3	1.46	0.16	1.3
T1-5	47,000	8.6	17.3	2.01	0.23	4.0
Average	45000	6.5	11.2	1.68	0.18	2.1
Std. dev.	1581	1.9	4.9	0.25	0.04	1.8
CV	0.04	0.30	0.44	0.15	0.21	0.89

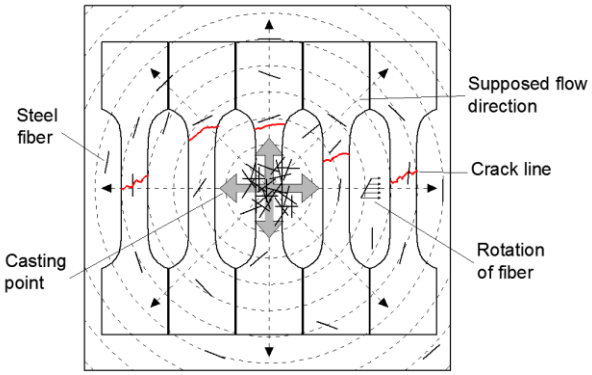

Fig.6 Schematic view of fiber distribution in the plate and crack positions of dumbbell specimens

3.2 Uniaxial tensile response based on inverse analysis from 4PBT

Fig.7 presents the bending behavior from 4PBT in terms of force-deflection curves, in which the black thick curve is the average curve. The results are more stable with little scatter, compared with those from uniaxial DDT. This is caused by the fact that the plate specimens for 4PBT were cast in molds individually, resulting in relatively similar fiber distribution.

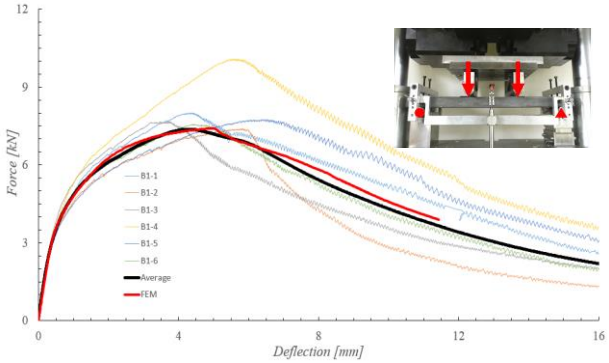

Fig.7 Bending response from 4PBT

The inverse analysis of 4PBT results was performed to evaluate the tensile response of UHPFRC indirectly based on non-linear Finite Element Method (FEM). A 2D FEM model was built using the non-linear FE analysis software DIANA (smeared crack model), targeting at simulating the bending behavior of the 4PBT in terms of force-deflection response and cracking pattern. The best results of FEM model fitting with the average tested response is shown in Fig.7, as indicated by the red thick line. A very close fit is achieved with the FEM model. The corresponding uniaxial tensile law is summarized in Fig.9 and Tab.2.

3.3 Biaxial tensile response based on inverse analysis from ring-on-ring test

The biaxial flexural response of four UHPFRC circular slabs from ring-on-ring tests are presented in terms of force vs. deflection of the center point (F - δ), as shown in Figure 8. For better comparison, the force was calculated considering a geometry factor that accounts for the precise slab thickness. The value of the geometry factor equals to $(h/h_i)^3$, where h is the nominal thickness (50 mm) and h_i is the measured thickness of each slab. The latter item was measured by DIC on bottom surface, excluding the deformation of the rubber pad measured from three LVDTs on the top surface. It is obvious that all slabs showed consistent flexural response, in particular, before the formation of macrocracks and with little scatter.

Similarly, in order to determine the biaxial tensile response of UHPFRC, the inverse analysis of the ring-on-ring test results were conducted by means of 3D FE models using DIANA. Considering the random fiber distribution in the slab, the full scale of the slab element was modeled, and the smeared crack concept was adopted. The modeling results with best fitting of F-δ curve for the average tested response is presented in Fig.8 (thick red line), where a very close fit is achieved. The corresponding biaxial tensile law is summarized in Fig.9 and Tab.2.

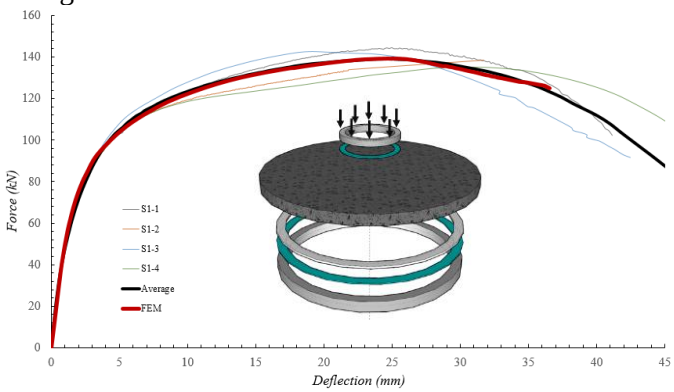

Fig.8 Biaxial flexural response from the ring-on-ring tests

4. COMPARISON & DISCUSSION

Finally, all the tensile laws under uniaxial or biaxial stress condition from experimental results and inverse analysis by FEM models, as well as the corresponding tensile parameters, are summarized in Fig.9 and Tab.2, respectively.

The uniaxial tensile response from DDT exhibits significantly more scatter and lower performance than that from 4PBT by inverse analysis. The large scatter in DTT results can be attributed to the variable fiber distribution in different dumbbell specimens that were extracted from different position of square plate, as described in section 3.1 and Fig.6. The slightly higher values for the tensile behavior as obtained from the 4PBT may be due to the fact that the plates with lower thickness were cast in molds individually, leading to preferable fiber distribution in critical loading area. Based on previous study [15], the average fiber orientation factor (μ_0) and efficiency factor (μ_1) in a layer of 50mm and 30mm of UHPFRC are listed in Table 2, respectively. Thus, considering the fiber distribution factors (μ_0 & μ_1) in the specimens, the 4PBT results are consistent with DTT results in terms of ultimate strength f_{Utu}. Thus, for comparison, the representative uniaxial tensile behavior from the 4PBT is determined by considering μ_0 and μ_1. It should be noted that no fracture zone appeared within or quite near the pouring zone (assuming random fiber distribution without flowing effect) in the large square plate for the DTT, suggesting that the tensile response from this area cannot be obtained directly (Fig. 6). Accordingly, the response of the five tested dumbbell specimens in DTT may not characterize the variability of the tensile behavior in the large square plate precisely, and the average response cannot be representative.

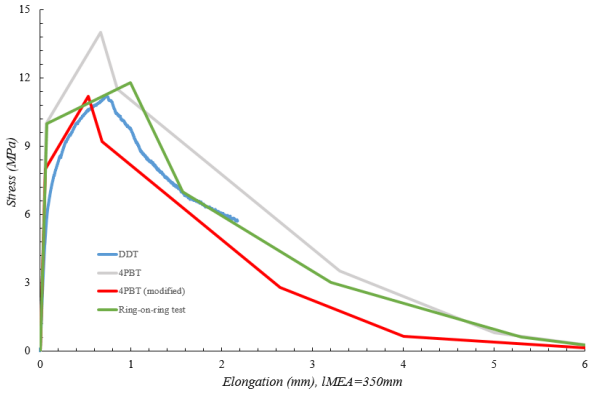

Fig.9 Tensile responses from different test methods

Tab.2 Tensile parameters from different test methods

Test Method	E_U [MPa]	f_{Ute} [Mpa]	f_{Utu} [Mpa]	f_{Utu}/f_{Ute}	ε_{Ute} [‰]	ε_{Utu} [‰]
DDT	45,000	6.50	11.20	1.68	0.18	2.10
4PBT	51,000	10.00	14.00	1.40	0.20	1.90
4PBT (((modified)	51,000	8.33	11.67	1.40	0.16	1.52
Ring-on-ring test	50,000	10.00	11.80	1.18	0.20	2.85

Note: For h=50mm, μ_0=0.53~0.60, μ_1=0.93; for h=30mm, μ=0.61~0.68, μ_1=0.95

According to Fig.9 and Tab.2, the values of f_{Utu} are similar for both the uniaxial and biaxial stress state, although the result from the ring-on-ring test is slightly higher. This may be because all the test methods provide the tested specimens with a certain area of maximally uniform stress, allowing for the microcracks to initiate and the macrocracks to localize in the weak zone with unfavorable fiber distribution. Additionally, since much more fibers in different directions contributed to the bridging and debonding effect in biaxial condition, offering considerably higher ductility and toughness with larger elongation, significant improve of ε_{Utu} and softening behavior are observed, compared with those under uniaxial condition, where fibers perpendicular to the loading direction have no effect. This difference is also explained by the different crack patterns due to stress states, as described in previous study [16]: more densely distributed microcracks and multiple localized macrocracks were produced in circular slabs under biaxial condition, while only one or two macrocracks were observed in dumbbell specimens and small plates under uniaxial condition. This implies that much more fracture energy was consumed to generate new cracks under biaxial condition

5. CONCLUSIONS

This study investigates the tensile behavior of UHPFRC “Holcim707©” under uniaxial and biaxial stress conditions by means of DDT, inverse analysis of 4PBT and ring-on-ring tests using FEM models. The results from the experimental campaign suggest that the tensile response of UHPFRC is not an intrinsic property and depends on several factors, including the specimen geometry, flow regime of fresh mixture during casting and stress condition.

The research findings from this study are presented as follows:

(1) The ring-on-ring tests using circular slab yield the most reliable results with little scatter, despite being the easiest test to perform among all the presented tests in this study, could be regarded as a valuable biaxial test method.

(2) The tensile responses from DTT strongly depend on the position of extracted specimens in the original square plate, showing large variability. The fracture zones of the five dumbbell specimens imply that fibers tend to align perpendicularly to the flow direction, resulting in a radial fiber distribution mode in the large plate.

(3) The inverse analysis by means of FEM models has been applied successfully to determine the tensile response of UHPFRC either in the 4PBT or ring-on-ring test. The results from FEM models and tests coincide well in terms of average force-deflection response.

(4) The values of the tensile strength f_{Utu} are similar for both the uniaxial and biaxial stress states. This may be because the microcracks could initiate and macrocracks could localize in the weak zone within the uniform stress areas of the specimens in all the different test methods.

(5) A significant improvement of the strain-hardening and strain-softening behavior is observed under biaxial stress conditions, compared to those from uniaxial conditions. These differences can be explained by more significant bridging and debonding effect due to the fibers being present in the different directions, as well as by the larger fracture zone with more frequent microcracks and macrocracks under biaxial stress conditions.

REFERENCES

[1] J. Kim, D.J. Kim, S.H. Park, G. Zi, Investigating the flexural resistance of fiber reinforced cementitious composites under biaxial condition, Composite Structures. 122 (2015) 198–208.

[2] C. ASTM, 1499-05. Standard test method for monotonic equibiaxial flexural strength of advanced ceramics at ambient temperature, ASTM International, West Conshohocken, Pennsylvania. (2009).

[3] G. Zi, H. Oh, S.-K. Park, A novel indirect tensile test method to measure the biaxial tensile strength of concretes and other quasibrittle materials, Cement and Concrete Research. 38 (2008) 751–756.

[3] O. Ekincioglu, A discussion of paper "A novel indirect tensile test method to measure the biaxial tensile strength of concretes and other quasibrittle materials" by G. Zi, H. Oh, S.K. Park, Cement and Concrete Research. 40 (2010) 1769–1770.

[5] J. Kim, D.J. Kim, G. Zi, Improvement of the biaxial flexure test method for concrete, Cement and Concrete Composites. 37 (2013) 154–160.

[6] D.-Y. Yoo, G. Zi, S.-T. Kang, Y.-S. Yoon, Biaxial flexural behavior of ultra-high-performance fiber-reinforced concrete with different fiber lengths and placement methods, Cement and Concrete Composites. 63 (2015) 51–66.

[6] D.-Y. Yoo, N. Banthia, G. Zi, Y.-S. Yoon, Comparative Biaxial Flexural Behavior of Ultra-High-Performance Fiber-Reinforced Concrete Panels Using Two Different Test and Placement Methods, Journal of Testing and Evaluation. 45 (2017) 20150275.

[8] H. Neuber, Der zugbeanspruchte Flachstab mit optimalem Querschnittsübergang, Forschung Im Ingenieurwesen. 35 (1969) 29–30.

[9] S.D.P. Benson, B.L. Karihaloo, CARDIFRC®-Development and mechanical properties. Part III: Uniaxial tensile response and other mechanical properties, Magazine of Concrete Research. 57 (2005) 433–443.

[10] Technical Leaflet SIA 2052 UHPFRC – Materials, design and construction, March 2016. (in German and French; for English translation contact: eugen.bruehwiler@epfl.ch).

[11] E. Denarié, L. Sofia, E. Brühwiler, Characterization of the tensile response of strain hardening UHPFRC - Chillon Viaducts, AFGC-ACI-Fib-RILEM Int. Symposium on Ultra-High Performance Fibre-Reinforced Concrete, UHPFRC 2017. (2017).

[10] A. Blanco, Characterization and modelling of SFRC elements, TDX (Tesis Doctorals En Xarxa). (2013). (accessed July 28, 2016).

[11] D.-Y. Yoo, N. Banthia, Mechanical properties of ultra-high-performance fiber-reinforced concrete: A review, Cement and Concrete Composites. 73 (2016) 267–280.

[12] A. Abrishambaf, M. Pimentel, S. Nunes, Influence of fibre orientation on the tensile behaviour of ultra-high performance fibre reinforced cementitious composites, Cement and Concrete Research. 97 (2017) 28–40.

[13] M. Bastien-Masse, E. Denarié, E. Brühwiler, Effect of fiber orientation on the in-plane tensile response of UHPFRC reinforcement layers, Cement and Concrete Composites. 67 (2016) 111–125.

[16] X. Shen, E. Brüehwiler, Flexural quasi-static behavior of UHPFRC circular slab specimens, AFGC-ACI-Fib-RILEM Int. Symposium on Ultra-High Performance Fibre-Reinforced Concrete, UHPFRC 2017. (2017).